

Title:

*in*Pentosomes: an innovative nose-to-brain pentamidine delivery blunts MPTP parkinsonism in mice

Author names:

Rinaldi F*¹, Seguella L*², Gigli S*², Hanieh PN¹, Del Favero E³, Cantù L³, Pesce M⁴, Sarnelli G⁴, Marianecci C^{1°}, Esposito G^{2§}, Carafa M^{1§}.

*these authors equally contributed as first author

§ these authors equally contributed as last author

Affiliations:

¹Department of Drug Chemistry and Technology, University of Rome "Sapienza", Rome, Italy.

²Department of Physiology and Pharmacology "V. Erspamer", Sapienza University of Rome, Rome, Italy.

³ Department of Medical Biotechnologies and Translational Medicine, University of Milan, Italy

⁴ Department of Clinical Medicine and Surgery, University of Naples 'Federico II', Naples, Italy.

Author for correspondence

[°] Dr. Carlotta Marianecci, Department of Drug Chemistry and Technologies, Sapienza University of Rome, Piazzale A. Moro, 5 - 00185 Rome, Italy. Email: carlotta.marianecci@uniroma1.it

Abstract

Preclinical and clinical evidences have demonstrated that astroglial-derived S100B protein is a key element in neuroinflammation underlying the pathogenesis of Parkinson's disease (PD), so much as that S100B inhibitors have been proposed as promising candidates for PD targeted therapy. Pentamidine, an old-developed antiprotozoal drug, currently used for pneumocystis carinii is one of the most potent inhibitors of S100B activity, but despite this effect, is limited by its low capability to cross blood brain barrier (BBB). To overcome this problem, we developed a non-invasive intranasal delivery system, chitosan coated niosomes with entrapped pentamidine (*inPentasomes*), in the attempt to provide a novel pharmacological approach to ameliorate parkinsonism induced by subchronic MPTP administration in C57BL-6J mice. *inPentasomes*, prepared by evaporation method was administered daily by intranasal route in subchronic MPTP-intoxicated rodents and resulted in a dose-dependent manner (0.001-0.004 mg/kg) capable for a significant Tyrosine Hydroxylase (TH) positive neuronal density rescue in both striatum and substantia nigra of parkinsonian mice. In parallel, *inPentasomes* significantly decreased the extent of glial-related neuroinflammation through the reduction of specific gliotic markers (Iba-1, GFAP, COX-2, iNOS) with consequent PGE₂ and NO₂⁻ release reduction, in nigrostriatal system. *inPentasomes*-mediated S100B inhibition resulted in a RAGE/NF-κB pathway downstream inhibition in the nigrostriatal circuit, causing a marked amelioration of motor performances in intoxicated mice. On the basis of our results, chitosan coated niosomes loaded with pentamidine, the *inPentosome* system, self-candidates as a promising new intranasal approach to mitigate parkinsonism in humans and possibly paves the way for a possible clinical repositioning of pentamidine as anti-PD drug.

Keywords: pentamidine; Parkinson's disease; chitosan coated niosomes; nose-to-brain delivery; neuroinflammation; S100B-pentamidine inhibition.

Abbreviations: PD: Parkinson disease; ANOVA: Analysis of variance; EDTA: Ethylen-diaminetetraacetic acid; ELISA: Enzyme-linked immunosorbent assay; CNS: Central nervous system; GFAP: Glial fibrillary acidic protein; iNOS: Inducible nitric oxide synthase; TH :Tyrosine hydroxylase; NO: Nitric oxide; NO₂⁻: Nitrite; TNF-α: Tumor necrosis factor-α; IL-1β: Interleukin-1β; RAGE: Receptor for advanced glycation end-products; NF-κB: Nuclear factor kappa-B; BBB: Blood

brain barrier; IN: Intranasal; NSV: Non-ionic surfactant vesicles; DCP: Dicetyl phosphate; PBS: Phosphate buffer solution; MPTP: 1-Methyl-4-phenyl-1,2,3,6-tetrahydropyridine hydrochloride; ABC: Vectastain avidin-conjugated peroxidase complex; Iba-1: Ionized calcium-binding adapter molecule 1; COX-2: Cyclooxygenase 2; aCSF: Artificial cerebrospinal fluid; SDS: Sodium dodecyl sulphate; PGE₂: Prostaglandin E2

Introduction

Parkinson's disease (PD) is a complex, multifactorial neurodegenerative disease characterized by motor abnormalities, bradykinesia, tremor rest and muscular rigidity [1]. At histological view, accumulation of aggregated α -synuclein cores [2] accompanied to massive loss of dopaminergic neurons in the *substantia nigra pars compacta* typically feature PD brains [3, 4]. Despite a multifactorial and still to a large extent unknown exact etiopathogenesis, a large number of studies have highlighted nigro-striatal neuroinflammation a key event in parkinsonian neurodegeneration [4].

Following neurological insults, astrocytes and microglia are the main important inducers of a dynamic neuroinflammatory response in the brain termed reactive gliosis that is commonly observed in both post-mortem PD brains and in PD experimental models. Reactive gliosis has been highlighted as a key event in aggravating neuronal degeneration because activated astrocytes and microglia express a broad array of neurotoxic molecules, including pro-inflammatory cytokines and mediators, such as tumor necrosis factor- α (TNF- α), interleukin-1 β (IL-1 β) and nitric oxide (NO) ([5, 6] in addition to reactive oxygen and nitrogen species. Among the plethora of signalling molecules which are released during neuroinflammation related to PD, astrocyte-deriving S100B protein appears as a key molecule that triggers and spreads the gravity of the disease. S100B is a 20 kDa, diffusible, Ca⁺⁺/Zn⁺⁺/p53-binding protein that may profoundly affect neuronal survival depending upon its concentration in the extracellular milieu. While physiological (nanomolar) S100B concentration account for neuronal development, plasticity, and damage repair [7] its aberrant (micromolar) secretion observed in reactive gliosis in PD parallels is not a bystander event, but actively participates to the aggravation of disease symptoms [8]. In these conditions, increased level of S100B accumulates at receptor for advanced glycation end-products (RAGE) site and nuclear factor-kappaB activation [9] and significantly correlate to neuroinflammation

aggravation, nigrostriatal dopaminergic loss and illness progression. S100B thus plays a prominent role in PD pathogenesis [8, 10] and innovative therapeutic approaches based on S100B inhibition may represent a new pharmacological intervention strategy for PD.

In this sense, the old-developed antiprotozoal drug pentamidine appears as a very promising candidate. Beyond its antiprotozoal activity, pentamidine inhibits reactive gliosis and display neuroprotective effects in vitro [11] and, interestingly, in Alzheimer's disease in vivo model [12] has proved to be one of the most potent inhibitors of S100B protein acting at its $\text{Ca}^{+2}/\text{Zn}^{+2}$ -p53 binding site of the protein, inhibiting S100B effects on RAGE [12, 13]. Despite such huge potentialities, pentamidine has not yet been rapidly tested as a possible new PD-drug since its unfavorable pharmacokinetic profile due its low capability to cross the blood brain barrier (BBB). To overcome these restrictions on the drug use, an innovative pharmaceutical strategy is represented by intranasal (IN) drug delivery by chitosan coated niosomes.

IN delivery of drugs is a non-invasive and highly-efficient route of administration of charged and/or high molecular weight drugs that, once absorbed by nasal mucosa epithelium, can reach the CNS exploiting the olfactory and trigeminal neural pathways and by this way, through a direct connection between the nasal cavity and the brain [14]. This provides in the same time significant drug concentration raise in the CNS, and also determines a rapid adsorption of carried molecules (less than 10 minutes) from olfactory mucosa to brain parenchyma [15]. To strength this approach, niosomes, also called non-ionic surfactant vesicles (NSV), as nanometric vesicles consisting of an aqueous core and one or multiple surfactant bilayers have been in this study considered as nose to brain delivery systems for pentamidine to avoid passage through the BBB. Niosomal vesicles are mainly composed of non-ionic surfactants (e.g. Tween 20) coupled to cholesterol and charged molecules (e.g. dicetyl phosphate) to increase bilayer stability [16, 17].

To strength the efficacy of niosomes, chitosan a linear polysaccharide composed of randomly distributed β -(1 \rightarrow 4)-linked D-glucosamine (deacetylated unit) and N-acetyl-D-glucosamine may increase olfactory mucosal absorption, due its capability to interact with mucin the main component of nasal mucus layer and it acts prolonging the contact time between the drug and mucosa itself [18].

The resulting formulation, obtained by the coating of negatively charged niosomal surface with positively charged chitosan for pentamidine delivery *in vivo*, has here indicated as *inPentasomes*. On the basis of these considerations, the present study aims at evaluating the effect of: (1) chitosan coating and pentamidine loading on niosomal structure, (2) *inPentasomes* delivery in well-validated mice model of PD, resembled by subacute MPTP intoxication in C57BL/6 mice, (3) the beneficial effect of such approach to favour pentamidine release into mice brain to inhibit reactive gliosis and neuroinflammation at nigrostriatal site exploiting pentamidine capability to inhibit S100B/RAGE signaling, and (4) relative dopaminergic rescue in the *nigra* of MPTP intoxicated animals with consequent amelioration PD-symptoms severity *in vivo* by *inPentasomes*.

2.1 Materials and animals

Polysorbate 20 (Tween 20), Dicetyl phosphate (DCP), Cholesterol (Chol), Hepes salt {N-(2-hydroxyethyl) piperazine-N'-(2-ethanesulfonic acid)}, Sephadex G75, Calcein, Chitosan (low molecular weight), phosphate buffer solution (PBS), MPTP (1-Methyl-4-phenyl-1,2,3,6-tetrahydropyridine) hydrochloride, ethanol, xylene and eukitt were purchased from Sigma-Aldrich (Milan, Italy). Vectastain avidin-conjugated peroxidase complex (ABC) Kit and DAB Substrate Kit for peroxidase were purchased from Vector Laboratories (Burlingame, CA, USA). Mouse anti-iNOS and mouse anti-tyrosine hydroxylase were purchased from Novus biologicals (Abingdon, UK). Rabbit anti-GFAP, rabbit anti-RAGE, rabbit anti-S100B, rabbit anti-phospho p38 mitogen activated protein kinases (MAPK), rabbit anti-total p38MAPK, mouse anti-NF- κ B p50, rabbit anti-NF- κ B p65 and mouse anti-Iba-1 were from Abcam (Cambridge, UK). Rabbit anti-COX-2 was purchased from Cell Signaling Technology (Danvers, MA, USA). Mouse anti- β -actin was purchased from Santa Cruz Biotechnology (Santa Cruz, CA, USA). Normal donkey serum, secondary antibodies conjugated to horseradish peroxidase (HRP) and biotinylated goat anti-mouse/rabbit IgG antibody were purchased from Jackson ImmunoResearch Laboratories (West Grove, PA, USA). Chemiluminescence detection reagents were purchased from Advansta (Menlo Park, CA, USA). ELISA kit was purchased from BioVendor (Brno, Czech Republic). All other products and reagents were of analytical grade.

Eight-weeks old male C57Bl/6J mice (Charles River, Calco, Lecco, Italy) were used for the experiments. Animals were housed at 22°C controlled-temperature under 12-h dark/light cycle with *ad libitum* access to food and water. Animal care and procedures were in compliance with

the IASP and European Community (EC L358/1 18/12/86) guidelines on the use and protection of animals in experimental research.

*2.2. Preparation and characterization of *inPentasomes**

1.2.1. Preparation and purification of Pentasomes

The thin layer evaporation method was used to prepare niosomal vesicles from Tween 20. In the sample, the surfactant: DCP: cholesterol molar ratios are respectively 7,5mM: 7,5mM: 15mM. All the vesicle constituents were firstly dissolved in an organic mixture (CH₃OH/CHCl₃ 3/1 v/v), then solvent was removed under vacuum. The obtained "film" was hydrated with 5 ml of pentamidine 5 mg/ml solution. The multilamellar vesicular suspension was vortexed for about 5 minutes and then sonicated (5 minutes, 16% amplitude and 60°C) using a microprobe operating at 20 kHz (VibraCell-VCX 400-Sonics, Taunton, MA, USA). The unilamellar vesicle suspension was purified by gel permeation chromatography using SephadexG75 (glass column of 50 x 1.2 cm) using Hepes buffer as the eluent.

2.2.2. Chitosan solution preparation

The low molecular weight chitosan solution was obtained by solubilization of chitosan in acetate buffer solution (0.2 M, pH 4.4) after overnight stirring.

2.2.3. Preparation of coated Pentasomes

The chitosan-coated Pentasomes (*inPentasomes*) formation was promoted by adding 1ml of chitosan solution to an equal volume of uncoated Pentasomes. The obtained suspension was stirred for 3 h in a thermostatic water bath at 10 °C.

2.2.4. Dynamic Light Scattering and ζ-Potential Measurements

Pentasomes and *inPentasomes* mean diameters (Z-Average) and size distributions (polydispersity index, PDI) were measured at the temperature of 25 °C by means of the dynamic light scattering (DLS) technique, using a Malvern ZetaSizerNano 90S, equipped with a 5 mW HeNe laser (wavelength $\lambda = 632.8$ nm) and a digital logarithmic correlator. The normalized intensity autocorrelation functions were detected at a 90° angle and analyzed by using the Contin algorithm

[19] in order to obtain the decay time of the electric field autocorrelation functions. The decay time is used to obtain the distribution of the diffusion coefficient D of the particles, which can be converted into an effective hydrodynamic radius R_H using the Stokes-Einstein relationship $R_H = k_B T / 6\pi\eta D$, where $k_B T$ is the thermal energy and η the solvent viscosity. The values of the radii reported here correspond to the intensity weighted average [20].

The electrophoretic mobility measurements were carried out by means of the laser Doppler electrophoresis technique using the Malvern ZetaSizerNano 90S apparatus equipped with a 5mW HeNe laser. The mobility u was converted into the ζ -potential using the Smoluchowski relation $\zeta = u\eta/\epsilon$, where η and ϵ are the viscosity and the permittivity of the solvent phase, respectively [21].

2.2.5 Small angle x-ray scattering (SAXS)

SAXS experiments were performed at ID02 high-brilliance beamline (European Synchrotron Radiation Facility, ESRF, Grenoble, France). SAXS technique is suitable to study the structural properties of nanovectors on a local scale, between 1 and 60 nm, to access their internal arrangement [22, 23]. Plastic capillaries (ENKI, Italy) were filled with 30 μ l of sample solutions and buffer and mounted on a temperature-controlled holder ($T=25$ °C). The appropriate irradiation time was selected to avoid any radiation damage (0.1 s). For each sample, the scattered intensity at different scattering angles was acquired on a 2D detector, then angularly regrouped and subtracted for the background and buffer contributions. The intensity profile is reported as a function of the momentum transfer $q = (4\pi/\lambda)\sin(\theta/2)$ where θ is the scattering angle and $\lambda = 0.1$ nm the X-ray wavelength.

2.2.6. Determination of drug entrapment efficiency (EE)

Pentamidine entrapment efficiency in Pentasomes was determined using UV spectrophotometer. Spectrophotometric analyses were carried out at 270 nm, by means of a spectrophotometer (Perkin-Elmer, lambda 3a, UV-Vis spectrometer) equipped by 1.0 cm path-length quartz cells and drug EE was calculated as follows:

$$E.E = \frac{Drug_{Ent}}{Drug_{Tot}} \times 100$$

Results are the average of three different batches \pm standard deviation.

2.2.7. Pentasomes stability evaluation

To assess colloidal stability at different temperatures, the vesicle formulations were stored at 4 and 25 °C for a period of 90 days. Samples from each batch were withdrawn at definite time intervals (1, 30, 60 and 90 days) and the ζ -potential and the mean of hydrodynamic diameter of Pentasomes were determined as previously described. In order to study the biological stability of Pentasomes in presence of Human serum (HS) and artificial cerebrospinal fluid (aCSF), depending upon the experiments an opportune volume of HS or aCSF were added to vesicle suspensions until reached at 45% or 90% respectively.

2.2.8. inPentasomes bilayer fluidity determination

The fluidity of *inPentasomes* bilayer was determined by fluorescence anisotropy studies using DPH as fluorescence probe. DPH was added to vesicle composition at the final concentration of 2×10^{-3} M and to obtain DPH-labeled Pentasomes, DPH solution was added to the constituents and the fluorescent probe loaded vesicles were obtained by film technique as reported above. To avoid any experimental artifact, i.e. to allow the fluorescent probe disposition in the vesicle bilayer, samples were stored 3 h at room temperature before the fluorescence anisotropy experiments.

2.2.9. In vitro release study

The experiments were carried out using dialysis tubes (Molecular Weight cut-off 8000 and 5.5 cm² diffusing area) at 37°C in 90% artificial cerebrospinal fluid (CSF). The set-up was kept at T = 37°C by means of a temperature-controlled water bath, and the release medium was gently magnetically stirred during the experiment.

Sample volumes (1 mL) were withdrawn from the solution at specific time intervals to perform UV analyses and then re-inserted back in the external medium. Released pentamidine was detected by means of a spectrophotometer (Perkin-Elmer, lambda 3a, UV-vis spectrometer), as described above. Aliquots were analyzed immediately after sampling. All release experiments were carried out in triplicate. The values reported in the present paper represent the mean values and lay within 10% of the mean.

2.3. Pharmacological study of inPentasomes on MPTP-intoxicated mice

2.3.1. Experimental plan

Mice were randomly divided in the following experimental groups (n=8 each one): vehicle; MPTP group; MPTP group receiving daily *in*Pentosomes at increasing doses (0.001-0.004 mg/kg); MPTP receiving empty nanocarrier, as internal group. Experimental parkinsonism in mice was induced by a sub-acute model of MPTP toxicity, consisting in daily intraperitoneal injection of MPTP (25 mg/kg) for four consecutive days starting from day 1 according to Carta et al., [24]. In our experimental conditions, *in*Pentosomes was administered once a day via intranasal route from day 0 until day 5. Three days after last MPTP administration, at day 7, open-field test and pole test were assessed to evaluate parkinsonian symptoms severity in the different experimental groups. After behavioral tasks, animals were euthanized and brains isolated in order to perform immunoblot and immunohistological staining analysis, as described below.

2.3.2. Immunoblot

Post mortem striatal areas were gently dissected from mice and tissues were homogenized in ice-cold hypotonic lysis buffer to obtain cytosolic extracts. After protein quantification by Bio-Rad assay, an equal amount of protein (20 µg) underwent electrophoresis through a sodium dodecyl sulphate (SDS) polyacrilamide gel. Proteins were transferred onto nitrocellulose membrane, saturated for 1 h at room temperature with 5% (w/v) non-fat dry milk and then incubated overnight at 4°C with, depending upon the experiments, with rabbit polyclonal anti-RAGE (1:1000), rabbit polyclonal anti-S100B (1:100), rabbit monoclonal anti-phospho p38 mitogen activated protein kinases (MAPK) (1:1000), rabbit polyclonal anti-total p38MAPK (1:1000), mouse monoclonal anti-NF-κB p50 (1:1000), rabbit polyclonal anti-NF-κB p65 (1:6000), mouse anti-iNOS (1:1000), rabbit anti-GFAP (1:10000), mouse anti-Iba-1 (1:200), rabbit anti-COX-2 (1:1000), mouse anti-β-actin (1:1000). Membranes were then incubated for 1 h at room temperature with the specific secondary antibodies conjugated to horseradish peroxidase (HRP). Immune complexes were revealed by enhanced chemiluminescence detection reagents. Blots were thus analyzed by scanning densitometry (GS-700 imaging densitometer; Bio-Rad). Results were expressed as OD (arbitrary units; mm²) and normalized on the expression of the housekeeping protein β-actin.

2.3.3. Immunohistochemistry

In other set of experiments, after behavioral tests completion, mice were deeply anesthetized with an overdose of pentobarbital and perfused with 4% paraformaldehyde in 0.1 M PBS, pH= 7.4. Mice brains were gently removed and post-fixed for 24 h in paraformaldehyde and

transferred to a 25% sucrose solution in 0.1 M PBS for dehydration. After 3 days, brains were cut into 20 µm coronal sections cryostat (Thermo Scientific, Germany). Sections containing striatum or *substantia nigra* were subjected to immunostaining. Briefly, endogenous peroxidase activity was inhibited by incubation with 1.5% hydrogen peroxidase in methanol for 20 min. Then sections were blocked for 1 h at room temperature with 2% normal donkey serum in PBS and then incubated overnight at 4°C with mouse anti-tyrosine hydroxylase (1:500) or rabbit anti-GFAP (1:1000). After washing in PBS, sections were incubated with biotinylated goat anti-mouse/rabbit IgG antibody (1:1000) for 1 h at room temperature. The sections were subsequently washed and incubated with avidin-conjugated peroxidase complex for 1 h followed by PBS washing. The peroxidase reaction was performed using DAB peroxidase substrate kit accordingly to manufacturer's instructions. Sections were dehydrated in ethanol, cleared in xylene, and mounted with Eukitt mounting medium. Sections were analyzed with a microscope (Nikon Eclipse 326 80i) and images were captured by a high-resolution digital camera (Nikon Digital Sight DS-U1). Results were expressed as TH or GFAP relative optical density in striatum normalized on the vehicle group optical density. Otherwise, in *substantia nigra*, results were expressed as TH positive neurons number.

2.3.4. Enzyme-linked immunosorbent assay for PGE₂

Enzyme-linked immunosorbent assay (ELISA) for PGE₂ was carried out on brain tissue lysates according to the manufacturer's protocol. Absorbance was measured on a microtiter plate reader. PGE₂ level was determined using standard curves method.

2.3.5 Nitric oxide quantification

Nitric oxide (NO) was measured as nitrite (NO₂⁻) accumulation in brain tissue homogenates, by a spectrophotometer assay based on the Griess reaction [25]. Briefly, Griess reagent (1% sulphaniamide, 0.1% naphthylethylenediamine in H₃PO₄) was added to an equal volume supernatant and the absorbance was measured at 550 nm. Nitrite concentration (nM) was thus determined using a standard curve of NaNO₂.

2.3.6. Open-field test

Locomotor activity was assessed by using an open field apparatus, consisting of a 50 x 50cm light-gray opaque walls square arena with 50 cm wall's height according to Varga et al., [26]. The square arena was divided into 16 sub-squares. The test started by placing the mouse at the center of the arena and the number of line crossings (sub-squares boundaries crossing with both forepaws) was scored by a blinded observer during 6 min of observation. The results were expressed as average of movement frequency (number of crossing/time interval). After each test, the apparatus was thoroughly cleaned with cotton pad wetted with 70% ethanol.

2.3.7. Pole test

In order to evaluate the motor coordination, pole test was performed according to Venezia et al., [27]. Each animal was placed head upward on the top of a vertical rough-surfaced pole (8mm diameter; 50cm length) in their home cage to ensure and encourage the animal's return to a familiar environment. At day 0, the animals have been habituated to turn and climb down the pole and they were allowed to five trials. On the testing day, the time spent to completely turn orientation (T_{turn}) and to descend the pole (T_L) for each animal in completed five trials were evaluated. Animals were recorded via an overhead digital video camera and the results have been expressed as average T_{turn} and T_L time.

2.4. Statistical analysis

Results were expressed as mean \pm SEM of n experiments. Statistical analysis was performed using parametric one-way analysis of variance (ANOVA) and multiple comparisons were performed by Bonferroni's post hoc test; p values <0.05 were considered significant.

3. Results and discussion

The actual PD therapy is aimed to improve the quality of life of patients and despite to a broad spectrum of drugs, given as monotherapy or in combination, there is a substantial inefficiency to reverse the course of the pathology. The possibility to target neuroinflammation underlining PD with molecules capable to blunt astrocyte and microglia activation, has been proposed as a promising approach to delay neurodegenerative course [6]. Along this line, pentamidine has been re-sight in under a new light, beyond its antimicrobial effect, since it has been shown to inhibit S100B protein activity, a glial-derived protein that plays a crucial role in reactive gliosis and

neurodegeneration. Despite such interesting activity, pentamidine has an unfavourable pharmacokinetic profile because of its almost insignificant passage in the CNS. To this aim, in order to enhance the pentamidine BBB crossing and reduce the administrated dose and the relative degradation and secondary effects, we prepared a chitosan-coated niosomes for pentamidine suitable for intranasal administration (*in*Pentasomes).

Niosomes are surfactants vesicles obtained by the “film” method and composed by amphiphilic substances Tw20 and DCP. Cholesterol was also added into the formulation to improve the cohesion of the apolar portions of niosomal bilayer. This formulation was optimized with the addition of chitosan coating, which is a mucoadhesive agent widely used in nasal formulation and useful to stabilize vesicles [28, 29] (Table 1). Dynamic light scattering (DLS) analyses showed that *in*Pentasomes have an increased size in comparison with the uncoated vesicles (from 172 nm to 300 nm). Moreover, the innovative formulation is characterized by a positive ζ -potential value due to the positive charge of amino groups of chitosan responsible for the interaction with negative surface conferred by DPC in the uncoated vesicles. PDI values remains around 0,2 in both cases (data not shown) confirming the monodispersity of vesicle formulations. In a similar way, bilayer fluidity, microviscosity and polarity are not significantly affected by chitosan coating, as observed in Table 1.

Sample	Tw20 (mM)	DCP (mM)	Chol (mM)	EE%	Z-average (nm) \pm SD	ζ -Potential (mV) \pm SD	Fluidity (Anisotropy) AU	Polarity (I_{\parallel}/I_{\perp})	Microviscosity (I_E/I_3)
Pentasomes	7.5	7.5	15.0	24	172.0 \pm 3.9	-35.0 \pm 0.8	0.27	1.20	0.20
<i>in</i> -Pentasomes					300.7 \pm 17.2	+39.0 \pm 1.1	0.28	1.15	0.15

Table 1. Sample composition and chemical-physical properties. Results are expressed as means \pm SD (n = 3).

The structures of coated and uncoated niosomes were investigated performing Small-Angle X-ray Scattering (SAXS) analysis (Fig 1 Panel A). The scattered intensity profiles are characteristic for bilayer-type aggregates and the presence of peaks indicate that these structures are multilamellar. The q position of the intensity peaks is related to the characteristic interlamellar distance between

the adjacent bilayers inside the *in*Pentosomes ($d = 2\pi/q$). In the uncoated system the peak is around $q = 1 \text{ nm}^{-1}$, corresponding to an interlamellar distance of 6 nm. In the coated system the intensity peak moves to higher q values ($q = 1.17 \text{ nm}^{-1}$), corresponding to a shorter interlamellar distance, 5.4 nm. This effect is dictated by the addition of chitosan as the it is observed also in chitosan coated niosomes without pentamidine (Fig 1 Panel B) The addition of the chitosan solution induces a shrinkage of the aggregates, without any appreciable change in the thickness of each internal bilayer. Results indicate that chitosan covers the external surface of the *in*Pentosomes inducing a more compact internal structure related to the depletion of the water confined between the adjacent niosomal bilayers.

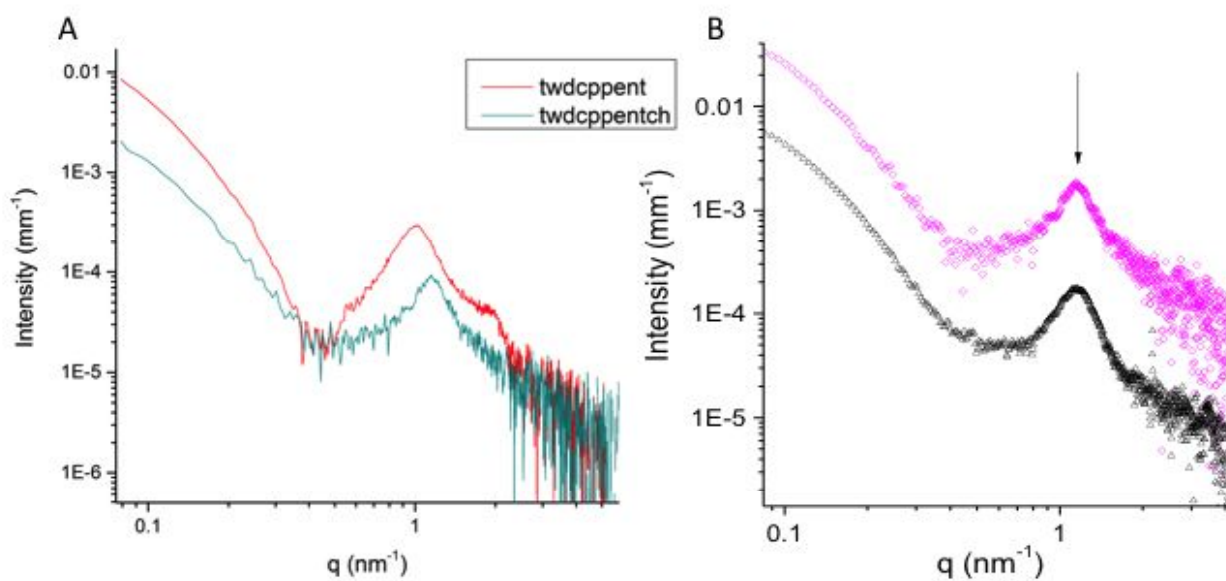


Fig.1. Small Angle X-ray Scattered intensity profiles.

Panel A: profiles of uncoated (blue open dots) and coated (magenta open diamonds) pentamidine loaded niosomes, vertically shifted for better clarity. Panel B: profiles of chitosan coated niosomes (black open triangles) and chitosan coated Pentosomes (magenta open diamonds), vertically shifted for better clarity. The position of the characteristic peak is the same, $q = 1.17 \text{ nm}^{-1}$ for both systems, corresponding to an interlamellar distance $d = 5.4 \text{ nm}$.

The chitosan coating does not vary the bilayer characteristics in terms of fluidity, microviscosity and polarity. As hypothesized, the polyelectrolyte/vesicle interactions are only surface electrostatic interactions and do not influence the bilayer structural order (Table 1). The anisotropy value gives information about bilayer fluidity; its value rises with the increase of rigidity. The value obtained for the two analysed samples is compatible with a quite rigid bilayer, according to SAXS results.

After intranasal administration it is expected that, the chitosan coating will remain adsorbed in the nasal cavity, while only the uncoated vesicles (Pentosomes) will be involved in the nasal mucosa crossing.

Studies on physical stability were also performed. *In*Pentosome showed a high colloidal stability when stored at 4°C in a time interval of 90 days, in terms of dimension and ζ -potential variations. (Fig 2 Panel A). The presence of chitosan increases the retention time of the formulation in the nasal cavity allowing the transport of the niosome across the nasal mucosa [30]. At this point, the uncoated niosome stability was evaluated at 37°C in aCSF. Pentosomes resulted immediately coated by aCSF proteins without any significant alterations in dimensions and ζ -potential within 180 min (Fig 2 Panel B).

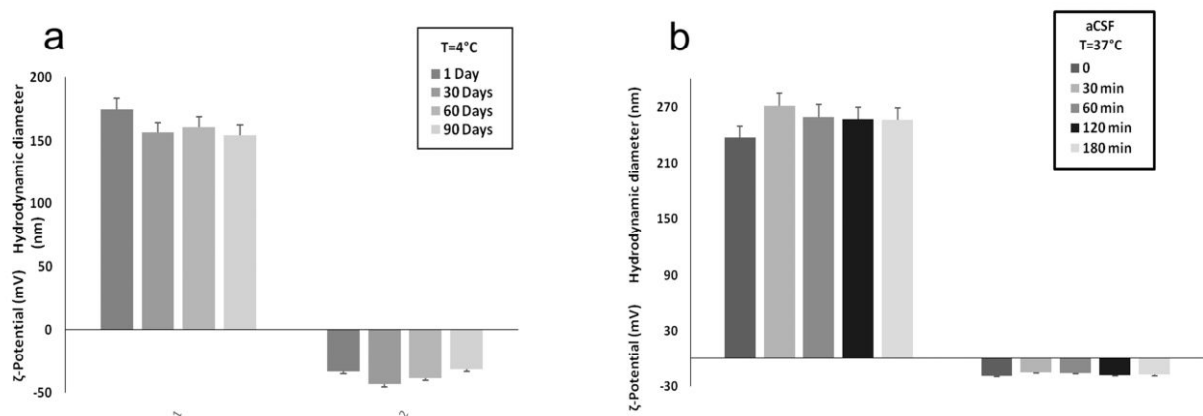


Fig.2. Stability of pentamidine loaded vesicles (Pentosomes).

Panel A: Shelf stability studies in terms of hydrodynamic diameter and z-potential value variations up to 90 days stored at 4°C. Panel B: Biological stability of the same sample in presence of aCSF up to 3 hours at 37°C. Results are expressed as means \pm SD (n = 3).

Along this line, analysis of pentamidine release in aCSF confirmed that the amount of the drug encapsulated in the formulation is entirely released within 4h (Fig 3), this was also demonstrated by the absence of niosomes in the acceptor compartment, after DLS analysis.

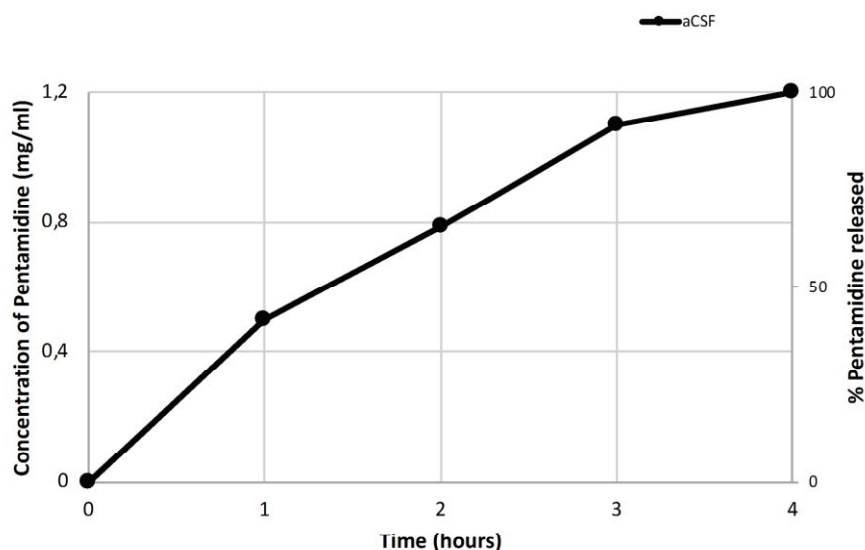


Fig.3. Release profile of pentamidine.

Pentamidine release by Pentasomes in aCSF at 37°C expressed as pentamidine concentration and % released pentamidine. Error bars are the same size or smaller than the symbols.

The physical-chemical characterization of *in*Pentosome highlighted the stability of the formulation and its suitability for brain delivery through the intranasal administration. On the basis of these results, the *in vivo* studies have demonstrated that the intranasal administration of *in*Pentosome lead to a marked improvement of PD-hallmarks and a significant reduction of neuroinflammation markers after 5 days of treatment in MPTP-intoxicated mice.

In pharmacological field, MPTP mouse model of PD is one of the most used animal models to study this neurodegenerative pathology [31]. In our experimental conditions, MPTP administration induced a marked dopaminergic neuronal loss in both striatum and *substantia nigra* areas (Fig. 4). Immunohistochemistry staining highlighted a significant reduction of TH positive cells in MPTP-treated mice versus vehicle group (-82% and -68%, respectively). Surprisingly, *in*Pentosomes via intranasal route was able to rescue the dopaminergic cellular density and TH positive cells in a dose-dependent fashion (0.001 mg/kg: +150% and +58%, respectively; 0.004 mg/kg: +405% and +174%, respectively; versus MPTP group). Conversely, the empty niosomes didn't show any significant improvement in TH cellular density within nigrostriatal axis following MPTP administration.

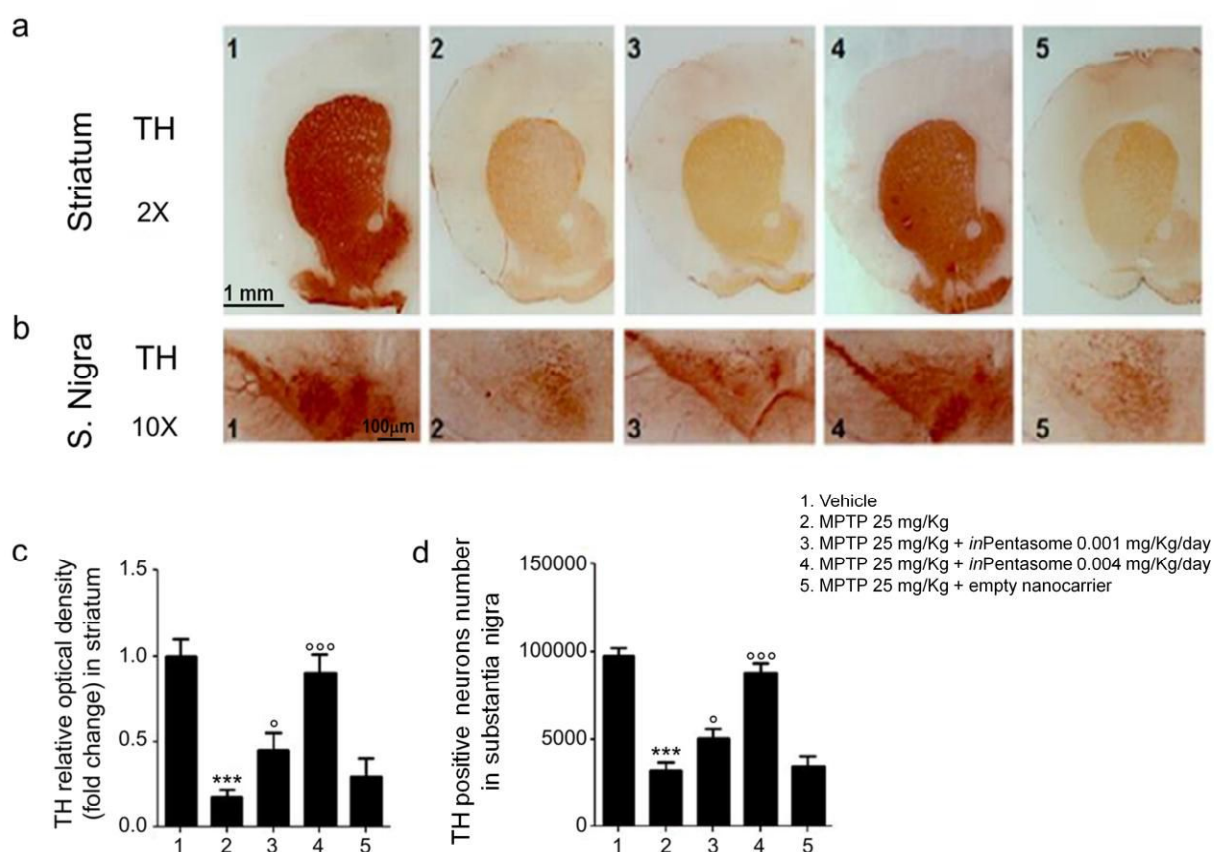


Fig 4. *InPentosomes* inhibit MPTP-induced dopaminergic neuronal loss in nigrostriatal areas.

The intranasal administration of *inPentosomes* (0.001-0.004 mg/kg) significantly and in dose-dependent manner increased dopaminergic cellular density and TH positive cells number in both striatum and substantia nigra of MPTP-treated mice (25 mg/kg) compared to vehicle group. Empty niosomes has not able to counteract MPTP-induced TH positive cells impairment. (A) The panel shows TH positive cells in striatum and (B) substantia nigra and (C, D) their respective quantification expressed as TH relative optical density and TH positive neurons number, respectively. Results are expressed as mean \pm SEM of $n=5$ experiments. *** $p < 0.001$ vs. vehicle group; ° $p < 0.1$ and °° $p < 0.001$ vs. MPTP group. Scale bar: 1 mm and 100 μ m for striatum and substantia nigra, respectively.

As previously anticipated, the hypothesis that this dopaminergic neuronal depletion is accompanied by a prominent neuroinflammation glia-mediated is widely accepted. To test whether *inPentosomes* efficacy was due to its ability to modulate neuroinflammation severity, astrogliosis and proinflammatory cytokines expression were evaluated (Fig. 5).

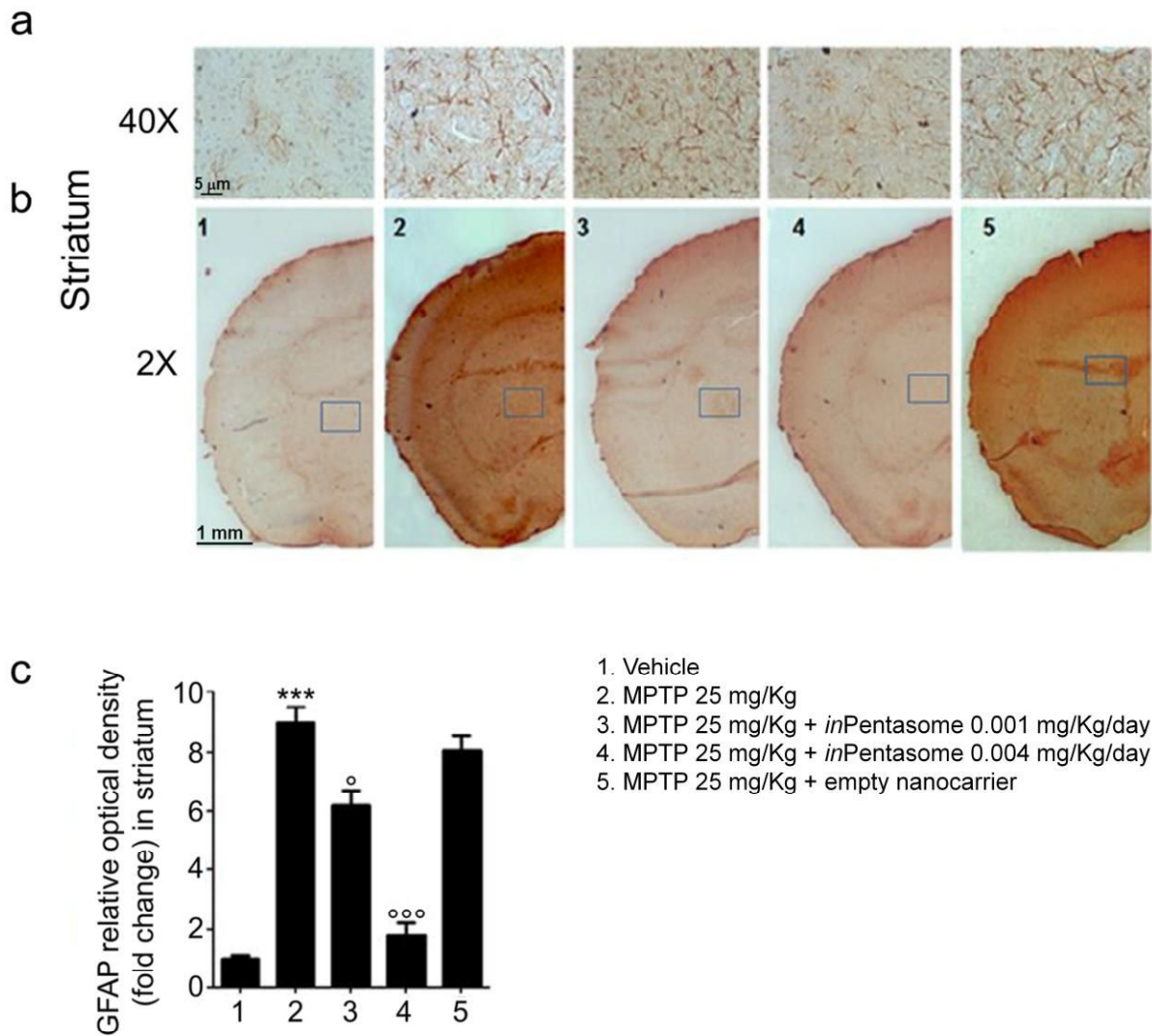


Fig 5. *In*Pentosomes reduces astrogliosis in striatum of MPTP-intoxicated mice.

(A, B) Immunohistochemistry staining showed that MPTP (25 mg/Kg) induced a marked increase of GFAP expression in striatum which was reduced in a dose-dependent fashion by intranasal administration of *in*Pentosomes (0.001-0.004 mg/kg). Empty niosomes administration failed to significantly affect GFAP up-regulation induced by MPTP administration. (C) Relative quantification of GFAP optical density. Results are expressed as mean \pm SEM of $n=5$ experiments. *** $p < 0.001$ vs. vehicle group; ° $p < 0.1$ and °°° $p < 0.001$ vs. MPTP group. *Scale bar*: 1 mm and 5 μ m at 2X and 40X, respectively.

Immunohistochemistry staining for GFAP showed a marked astrogliosis in the striatum of MPTP-treated mice brain compared to vehicle group (+800%). As expected, increasing doses of *in*Pentosome reduced significantly the optical density of GFAP (0.001 mg/kg: -32%; 0.004 mg/kg: -

80%, versus MPTP group), whereas the empty nanocarrier didn't affect the astroglial process MPTP-mediated.

Along this line, following MPTP treatment an increase of GFAP (+230%), COX-2 (+1450%), iNOS (+510%) and Iba-1 (+265%) protein expression was observed in brain tissues lysates, as well as nitrite (+855%) and PGE₂ (+430%) release (Fig. 6). Proinflammatory cytokines level was markedly reduced in presence of *in*Pentosome 0.001 mg/kg (GFAP: -27%; COX-2: -25% ; iNOS: -40% ; Iba-1: -24%; NO₂⁻: -38%; PGE₂: -29%; versus MPTP group) and 0.004 mg/kg (GFAP: -51%; COX-2: -55%; iNOS: -66%; Iba-1: -59%; NO₂⁻: -60%; PGE₂: -52%; versus MPTP group), but not with empty niosomes (Fig. 6).

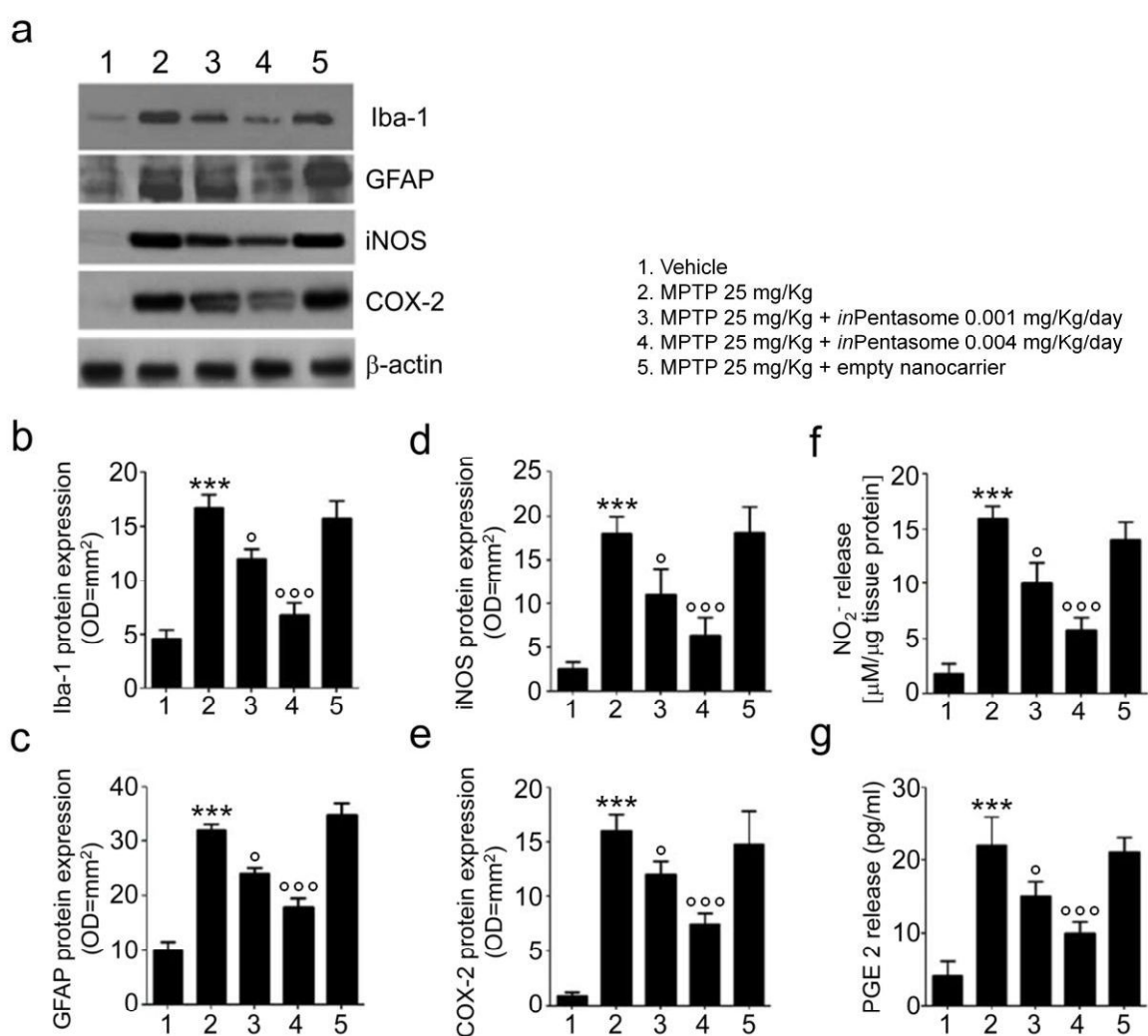


Fig 6. *In*Pentosomes reduce glial-related neuroinflammation markers in striatum of MPTP-intoxicated mice.

*In*Pentosomes (0.001-0.004 mg/kg) induced a significant and dose-dependent decrease of Iba-1, GFAP, iNOS and COX-2 protein expression, as well as PGE₂ and NO₂⁻ release in striatum deriving

from MPTP-intoxicated mice. Empty niosomes did not show any significant effects. (A) Immunoblot analysis showed representative immunoreactive bands of analyzed proteins and (B-E) their densitometric quantification (normalized against the expression of the housekeeping protein β -actin; OD= optical density in mm^2). (F, G) Levels of NO_2^- and PGE_2 in striatum homogenates. Results are expressed as mean \pm SEM of $n=5$ experiments *** $p < 0.001$ vs. vehicle group; ° $p < 0.1$ and °° $p < 0.001$ vs. MPTP group.

In the recent years, several evidences highlighted the leading role of astroglial-derived S100B protein in the neuronflammatory processes and development of different neurodegenerative disease, including PD, proposing the S100B inhibitors as new therapeutic tools in the attempt to slow or halt the disease course. Not by chance, it has been demonstrated that S100B protein levels are significantly higher in post-mortem *substantia nigra* and cerebrospinal fluid of PD patients than control tissues, underlining a close relationship between S100B overexpression with neuroinflammation, dopaminergic neuronal depletion and symptoms severity [8]. To confirm that, genetic models showed that S100B over-expression results in spontaneous parkinsonism in adult mice, while S100B^{-/-} mice display a less severe parkinsonism following MPTP administration, when compared to wild type mice [8, 10].

According to literature, in Figure 7 our results showed a significant increase in S100B protein expression at day 7 from MPTP injection (+450% versus vehicle). Similarly, we observed a considerable activation of the pathway responsible for S100B activity, represented by a marked increase in RAGE (+471%) protein expression, in the phosphorylation of p38MAPK (+4185%) and in the upregulation of NF- κ B activation marker p65 (+850%) and p50 (+633%), when compared to vehicle group. The identification of pentamidine as one of the most pharmacologically active inhibitors of S100B activity has provided a promising candidate for PD targeted therapy. Indeed, without affecting the S100B protein expression, *inPentosome* is able to inhibit its activity resulting in a significant decrease in RAGE (0.001 mg/kg: -40%; 0.004 mg/kg: -80%), p-p38 MAPK (0.001 mg/kg: -33%; 0.004 mg/kg: -70%), p65 (0.001 mg/kg: -34%; 0.004 mg/kg: -81%) and p50 (0.001 mg/kg: -32%; 0.004 mg/kg: -75%) protein expression in comparison with MPTP group. Once again, the empty niosomes did not exert any protective effect on MPTP intoxicated mice.

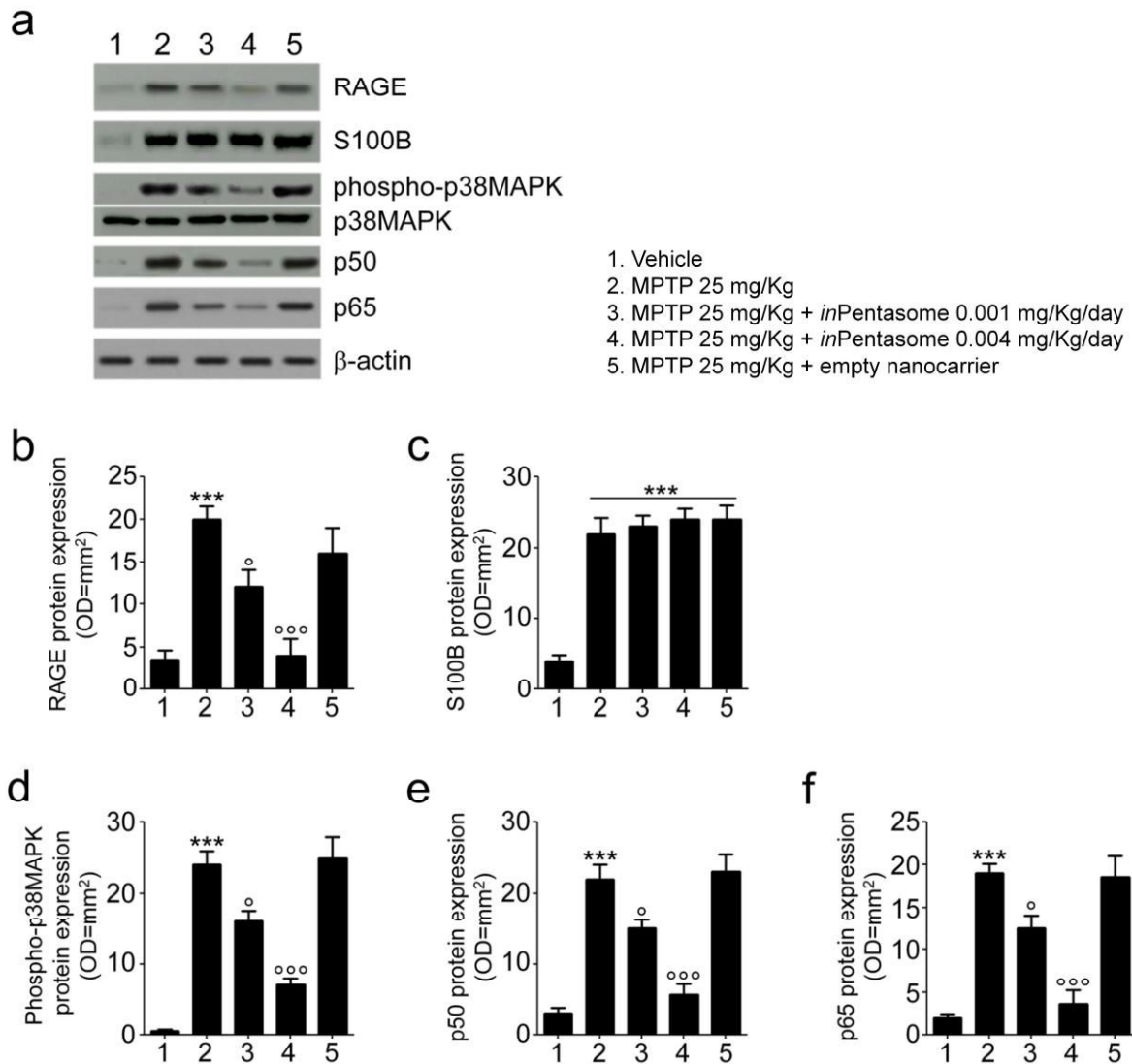


Fig 7. *InPentosomes* inhibited RAGE/NF- κ B pathway responsible for S100B proinflammatory activity.

Intranasal administration of *inPentosomes* (0.001 mg/kg-0.004 mg/kg) has resulted in a dose-dependent inhibition of RAGE/p38MAPK/NF- κ B downstream pathway responsible for S100B-induced neuroinflammation, but it was ineffective to reduce S100B protein expression. Empty niosomes did not induce any change in the above investigated parameters compared to MPTP group. (A) Relative quantification of corresponding immunoreactive bands and (B-F) their respective densitometric quantification (normalized against the expression of the housekeeping protein β -actin; OD=Optical Densitometry in mm²). Results are expressed as mean \pm SEM of $n=5$ experiments *** $p < 0.001$ vs. vehicle group; ° $p < 0.1$ and °° $p < 0.001$ vs. MPTP group.

Finally, motor dysfunctions were evaluated in order to test *inPentosome* efficacy on functional outcomes of PD. Open field locomotion test and pole test are behavioral assays well-established and widely used to determine locomotor activity and motor coordination, respectively. As reported in Figure 8, in our experimental model MPTP treatment caused a significant decrease of motor coordination, which was scored as number of line crossing in open-field test, in intoxicated mice versus vehicle group (-63%); intranasal administration of *inPentosome* improved animal performance in a dose-dependent manner (0.001 mg/kg: +60%; 0.004 mg/kg: +137%; versus MPTP group) whereas the empty niosomes didn't exert any amelioration. Similarly, both latency interval (T_L) and turning interval (T_{turn}), were significantly higher in MPTP-intoxicated mice undergone pole-test versus respective vehicle groups (T_L : +181%; T_{turn} : +220%). Conversely, increasing doses of *inPentosome* was able to revert such effect, decreasing both T_L (0.001 mg/kg: -37%; 0.004 mg/kg: -56%; versus MPTP group) and T_{turn} (0.001 mg/kg: -23%; 0.004 mg/kg: -58%; versus MPTP group) parameters. As expected, the empty vector didn't affect the MPTP-induced effects.

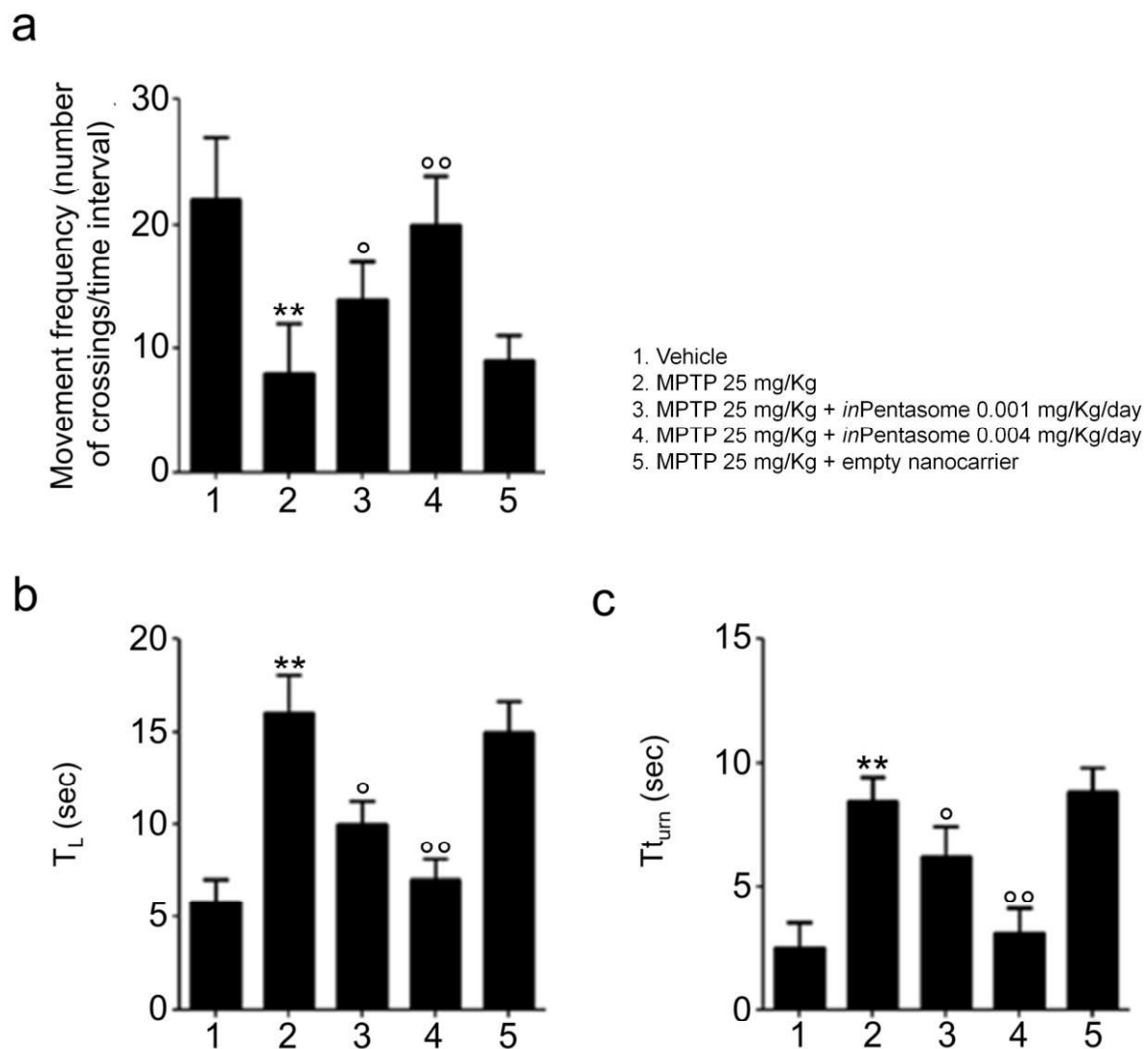


Fig 8. *InPentosomes* ameliorate motor deficits in MPTP-intoxicated mice.

(A) In MPTP-intoxicated mice (25 mg/Kg) a significant reduction of movement frequency was observed during open field test in comparison to vehicle group at day 7. Intranasal administration of *inPentosomes* (0.001 mg/kg-0.004 mg/kg) increased the number of line crossing in dose-dependent manner, while empty niosomes did not significantly affect the animal performance. (B-C) Even in pole test both latency interval (T_L) and turning interval (T_{turn}) were showed a significant increase in MPTP-intoxicated mice versus vehicle groups. *InPentosomes* treatment (0.001 mg/kg-0.004 mg/kg) was dose-dependent decreased these parameters, while empty niosomes lacks any significant effect on animal motor coordination in MPTP-treated mice. Results are expressed as mean \pm SEM of 8 per group ** $p < 0.01$ vs. vehicle group; $^{\circ}p < 0.1$ and $^{\circ\circ}p < 0.01$ vs. MPTP group.

Conclusions

This study proposed an innovative way of administration, such as intranasal one, of a novel chitosan coated niosomal formulation for pentamidine delivery in a murine model of PD. The drug encapsulation into niosomes, coated with mucoadhesive promoter chitosan, and administered through an intranasal route, guaranteeing high CNS localization and optimal concentrations of the drug in the brain. Moreover, this pharmaceutical formulation, called *inPentosome*, is characterized by high chemical stability, low toxicity and reduced costs. Because of its capability to inhibit glial-derived S100B activity, *inPentosome* was able to rescue the dopaminergic neuronal loss and reduce the severity of neuroinflammation occurred in the nigrostriatal pathway, leading to a significant improvement in parkinsonian motor dysfunctions. These evidences highlighted the efficacy of *inPentosome* in a mouse model of PD suggesting a promising and non-invasive brain delivery system for a future (*and possibly fast*) pentamidine repositioning as anti-PD drug in humans, thanks to an innovative nose-to-brain approach that maximize its efficacy and reduce dosage-related unwanted effects of this molecule.

Funding: this work was supported by Sapienza Ateneo funding “Multidisciplinari 2015” C26M15SP9F.

References

- [1] L.V. Kalia, A.E. Lang, Parkinson's disease, *The Lancet*, 386 (2015) 896-912. 10.1016/s0140-6736(14)61393-3.
- [2] F. Mori, Y.-S. Piao, S. Hayashi, H. Fujiwara, M. Hasegawa, M. Yoshimoto, T. Iwatsubo, H. Takahashi, K. Wakabayashi, α -Synuclein accumulates in Purkinje cells in Lewy body disease but not in multiple system atrophy, *Journal of Neuropathology & Experimental Neurology*, 62 (2003) 812-819.
- [3] H. Braak, E. Braak, Pathoanatomy of Parkinson's disease, *Journal of neurology*, 247 (2000) 113-110.
- [4] K. Kaur, J.S. Gill, P.K. Bansal, R. Deshmukh, Neuroinflammation-A major cause for striatal dopaminergic degeneration in Parkinson's disease, *Journal of the neurological sciences*, 381 (2017) 308-314.
- [5] P. Teismann, J.B. Schulz, Cellular pathology of Parkinson's disease: astrocytes, microglia and inflammation, *Cell and tissue research*, 318 (2004) 149-161.

- [6] Q. Wang, Y. Liu, J. Zhou, Neuroinflammation in Parkinson's disease and its potential as therapeutic target, *Translational Neurodegeneration*, 4 (2015) 19.
- [7] R. Bianchi, C. Adami, I. Giambanco, R. Donato, S100B binding to RAGE in microglia stimulates COX-2 expression, *Journal of leukocyte biology*, 81 (2007) 108-118.
- [8] K. Sathe, W. Maetzler, J.D. Lang, R.B. Mounsey, C. Fleckenstein, H.L. Martin, C. Schulte, S. Mustafa, M. Synofzik, Z. Vukovic, S100B is increased in Parkinson's disease and ablation protects against MPTP-induced toxicity through the RAGE and TNF- α pathway, *Brain*, 135 (2012) 3336-3347.
- [9] A. Villarreal, R.X. Aviles Reyes, M.F. Angelo, A.G. Reines, A.J. Ramos, S100B alters neuronal survival and dendrite extension via RAGE-mediated NF- κ B signaling, *Journal of neurochemistry*, 117 (2011) 321-332.
- [10] J. Liu, H. Wang, L. Zhang, Y. Xu, W. Deng, H. Zhu, C. Qin, S100B transgenic mice develop features of Parkinson's disease, *Archives of medical research*, 42 (2011) 1-7.
- [11] I.J. Reynolds, E. Aizenman, Pentamidine is an N-methyl-D-aspartate receptor antagonist and is neuroprotective in vitro, *Journal of Neuroscience*, 12 (1992) 970-975.
- [12] C. Cirillo, E. Capoccia, T. Iuvone, R. Cuomo, G. Sarnelli, L. Steardo, G. Esposito, S100B inhibitor pentamidine attenuates reactive gliosis and reduces neuronal loss in a mouse model of Alzheimer's disease, *BioMed research international*, 2015 (2015).
- [13] G. Esposito, E. Capoccia, G. Sarnelli, C. Scuderi, C. Cirillo, R. Cuomo, L. Steardo, The antiprotozoal drug pentamidine ameliorates experimentally induced acute colitis in mice, *Journal of neuroinflammation*, 9 (2012) 277.
- [14] W. Frey, Neurologic agents for nasal administration to the brain, *World Intellectual Property Organization*, 5 (1991) 89.
- [15] L.R. Hanson, W.H. Frey, Intranasal delivery bypasses the blood-brain barrier to target therapeutic agents to the central nervous system and treat neurodegenerative disease, *BMC neuroscience*, 9 (2008) S5.
- [16] F. Rinaldi, P.N. Hanieh, L.K.N. Chan, L. Angeloni, D. Passeri, M. Rossi, J.T.-W. Wang, A. Imbriano, M. Carafa, C. Marianecchi, Chitosan Glutamate-Coated Niosomes: A Proposal for Nose-to-Brain Delivery, *Pharmaceutics*, 10 (2018) 38.
- [17] F. Rinaldi, P.N. Hanieh, C. Marianecchi, M. Carafa, DLS Characterization of Non-Ionic Surfactant Vesicles for Potential Nose to Brain Application, *Nanosci. Nanometr.*, 1 (2015) 8-14.

- [18] L. Salade, N. Wauthoz, M. Vermeersch, K. Amighi, J. Goole, Chitosan-coated liposome dry-powder formulations loaded with ghrelin for nose-to-brain delivery, *European Journal of Pharmaceutics and Biopharmaceutics*, 129 (2018) 257-266.
- [19] S.W. Provencher, CONTIN: a general purpose constrained regularization program for inverting noisy linear algebraic and integral equations, *Computer Physics Communications*, 27 (1982) 229-242.
- [20] C. De Vos, L. Deriemaeker, R. Finsy, Quantitative assessment of the conditioning of the inversion of quasi-elastic and static light scattering data for particle size distributions, *Langmuir*, 12 (1996) 2630-2636.
- [21] S. Sennato, F. Bordi, C. Cametti, C. Marianecchi, M. Carafa, M. Cametti, Hybrid niosome complexation in the presence of oppositely charged polyions, *The Journal of Physical Chemistry B*, 112 (2008) 3720-3727.
- [22] G. Sandri, S. Motta, M.C. Bonferoni, P. Brocca, S. Rossi, F. Ferrari, V. Rondelli, L. Cantù, C. Caramella, E. Del Favero, Chitosan-coupled solid lipid nanoparticles: tuning nanostructure and mucoadhesion, *European Journal of Pharmaceutics and Biopharmaceutics*, 110 (2017) 13-18.
- [23] A. Clementino, M. Batger, G. Garrastazu, M. Pozzoli, E. Del Favero, V. Rondelli, B. Gutfilen, T. Barboza, M.B. Sukkar, S.A. Souza, The nasal delivery of nanoencapsulated statins—an approach for brain delivery, *International journal of nanomedicine*, 11 (2016) 6575.
- [24] A.R. Carta, A. Kachroo, N. Schintu, K. Xu, M.A. Schwarzschild, J. Wardas, M. Morelli, Inactivation of neuronal forebrain A2A receptors protects dopaminergic neurons in a mouse model of Parkinson's disease, *Journal of neurochemistry*, 111 (2009) 1478-1489.
- [25] M. Di Rosa, M. Radomski, R. Carnuccio, S. Moncada, Glucocorticoids inhibit the induction of nitric oxide synthase in macrophages, *Biochemical and biophysical research communications*, 172 (1990) 1246-1252.
- [26] D. Varga, J. Herédi, Z. Kánvási, M. Ruzska, Z. Kis, E. Ono, N. Iwamori, T. Iwamori, H. Takakuwa, L. Vécsei, Systemic L-Kynurenine sulfate administration disrupts object recognition memory, alters open field behavior and decreases c-Fos immunopositivity in C57Bl/6 mice, *Frontiers in behavioral neuroscience*, 9 (2015) 157.
- [27] S. Venezia, V. Refolo, A. Polissidis, L. Stefanis, G.K. Wenning, N. Stefanova, Toll-like receptor 4 stimulation with monophosphoryl lipid A ameliorates motor deficits and nigral neurodegeneration triggered by extraneuronal α -synucleinopathy, *Molecular neurodegeneration*, 12 (2017) 52.

- [28] I.F. Uchegbu, S.P. Vyas, Non-ionic surfactant based vesicles (niosomes) in drug delivery, *International journal of pharmaceutics*, 172 (1998) 33-70.
- [29] L. Illum, Nasal drug delivery—recent developments and future prospects, *Journal of controlled release*, 161 (2012) 254-263.
- [30] L. Casettari, L. Illum, Chitosan in nasal delivery systems for therapeutic drugs, *Journal of Controlled Release*, 190 (2014) 189-200.
- [31] G.E. Meredith, D.J. Rademacher, MPTP mouse models of Parkinson's disease: an update, *Journal of Parkinson's disease*, 1 (2011) 19-33.